European Journal of Medicinal Chemistry Reports 5 (2022) 100064

Contents lists available at ScienceDirect

European Journal of Medicinal Chemistry Reports

journal homepage: www.editorialmanager.com/ejmcr/default.aspx

Design of novel 4-maleimidylphenyl-hydrazide molecules displaying anti-inflammatory properties: Refining the chemical structure

Francis Cloutier [a], Yassine Oufqir [b], Laurie Fortin [b], Marie-France Leclerc [a], Julie Girouard [b], Heidar-Ali Tajmir-Riahi [a], Carlos Reyes-Moreno [b,**], Gervais Bérubé [a,*]

[a] *Laboratoire de Recherche en Chimie Médicinale (LRCM) et Groupe de Recherche en Signalisation Cellulaire (GRSC), Département de Chimie, Biochimie et Physique, Université du Québec à Trois-Rivières, Trois-Rivières, QC, Canada*

[b] *Laboratoire de Recherche en Oncologie et Immunobiologie (LROI) et Groupe de Recherche en Signalisation Cellulaire (GRSC), Département de Biologie Médicale, Université du Québec à Trois-Rivières, Trois-Rivières, QC, Canada*

ARTICLE INFO

Keywords:
Hydrazide derivatives
Acylation reaction
SAR study
Anti-inflammatory
Nitric oxide
Bladder cancer

ABSTRACT

The discovery of new drugs possessing multiple biological properties in a single molecular entity is a subject of considerable scrutiny by the scientific community. This strategy can lead to better drug candidates for the treatment of many diseases, including cancer. In our quest for a more efficient bladder cancer treatment, we recently identified a compound readily accessible from *para*-aminobenzoic acid that showed anti-inflammatory, anti-metastatic as well as anticancer activities. This unique compound called **DAB-1** can reduce the size of a tumor in an animal model by 90% within 25 days without apparent side effects. Its structure was modified to provide the molecule **2**, a second-generation molecule named **DAB-2-28,** with enhanced *in vitro* and *in vivo* biological properties compared to **DAB-1**. The prospect of lead optimization is significant. This manuscript describes the synthesis of **2** as well as several higher analogs and reports on their anti-inflammatory activity in addition to their *in vitro* biological potential against bladder cancer. Amongst the results, it was discovered that the substitution pattern on the hydrazide core significantly affects the anti-inflammatory potential of the molecules. In fact, all the mono-acylated hydrazide derivatives **1**, **5**, **7**, **9** were highly effective inhibiting the production of NO measured by the Griess reagents. By using the MTT assay, the same products displayed slightly lower toxicity (average 90% cell viability) on murine bladder cancer MB49-I cells in comparison to the reference **DAB-1** molecule (85%). The best mono-acylated derivative **1** showed about 83% NO production inhibition level in relation to the relative number of viable/proliferating cells, the results are disclosed herein.

1. Introduction

The global race to develop better anticancer drugs continues. Nowadays, much emphasis towards the development of anticancer molecules with greater selectivity and efficacy remains the subject of intense research activities [1–5]. The hybridization technique is largely used to gain greater specificity and activity on targeted cells [6–13]. Cancer is a complex disease that requires early detection and timely treatment for a positive outcome for the patient. As second leading cause of death globally, cancer accounts for an estimated 10 million deaths in 2021 as indicated by Global Cancer Statistics [14]. Worldwide, about 1 in 6 deaths is due to cancer. Bladder cancer (BCa) is not only an insidious health problem as it is frequently detected at a later stage but also quite difficult and costly to cure in comparison with other cancer types. In Canada, BCa is the fifth most frequent cancers with an estimated 12,500 predicted new cases representing 5.4% of all cancer cases after prostate cancer (10.5%), colorectal cancer (10.8%), breast cancer (12.2%) and lung and bronchus cancers (12.9%) [15]. In fact, BCa afflicts more frequently men than women with 9500 and 3000 new cases projected, respectively. For that reason, there is evidence that sex hormones,

Abbreviations: list: BCa, bladder cancer; NO, nitric oxide; PABA, *para*-aminobenzoic acid.

* Corresponding author.
** Corresponding author.
E-mail addresses: Francis.Cloutier2@uqtr.ca (F. Cloutier), Yassine.Oufqir@uqtr.ca (Y. Oufqir), Laurie.Fortin2@uqtr.ca (L. Fortin), Marie-France.Leclerc@uqtr.ca (M.-F. Leclerc), Julie.Girouard@uqtr.ca (J. Girouard), Heidar-Ali.Tajmir-Riahi@uqtr.ca (H.-A. Tajmir-Riahi), Carlos.Reyes-Moreno@uqtr.ca (C. Reyes-Moreno), Gervais.Berube@uqtr.ca (G. Bérubé).

https://doi.org/10.1016/j.ejmcr.2022.100064
Received 11 March 2022; Received in revised form 25 May 2022; Accepted 26 May 2022
Available online 29 May 2022

particularly testosterone and dihydrotestosterone play a crucial role in the initiation and development of this particular cancer [16].

Accumulating evidence suggests that chronic inflammation within the tumor microenvironment acts as an important mediator of neoplastic transformation and the progression of BCa by activating a series of inflammatory cells and signaling pathways [17–20]. Conceivably, targeting of pro-tumor inflammatory mediators and signaling pathways are presently proposed as a therapeutic option to prevent the progression of pre-invasive carcinoma and the treatment of late-stage cancer [19, 21–23]. Accordingly, some natural and synthetic anti-inflammatory agents that are currently tested in preclinical and clinical cancer trials are known to mediate their effects through inhibition of key pro-tumor inflammatory cytokines (IL6, TNFα), transcription factors (NFκB, STAT3) and soluble mediators (nitric oxide, prostaglandins) [19,23–27].

In this context, we have been investigating a hydrazide derivative named, **DAB-1** which was made from *para*-aminobenzoic acid (PABA) using a three-step reaction sequence (Fig. 1). This particular compound exhibited anti-inflammatory, anti-metastatic and anticancer activities. Our initial work shows that **DAB-1**, which is made of a maleimide and hydrazide moieties, demonstrated that both components of the molecule are essential for its activity [28]. Its interaction with transport proteins showed that drug-protein conjugation occurs mainly by ionic contacts [29]. In addition, *in vivo* biological evaluation of this molecule revealed that it produces its biological action through inhibition of TNFα/NFκB and iNOS/NO pathways [3]. In order to improve its biological potential, a new compound named **DAB-2-28** was synthesized and tested *in vitro* and *in vivo*. It was discovered that this molecule displayed less toxicity and higher potency than **DAB-1** in an animal model of BCa [30,31]. The synthesis and biological potential of higher analogs of **DAB-2-28** was deemed necessary for the discovery of even more potent compounds. In addition, it was of interest to explore the biological potential of the four possible acetylated products that can be obtained from **DAB-1**. This manuscript presents the results of this study.

2. Design and chemistry

The 4-maleimidylphenyl-hydrazide molecules are synthesized through a four-step reaction sequence starting from *para*-aminobenzoic acid. **DAB-1** is the cornerstone intermediate allowing the formation of **DAB-2-28** and higher homologs. Initially, the latter compound was obtained with only 18% yield along with some mono-acetylated derivatives [30]. Hence, it was decided to optimize its synthesis and to investigate the formation of the mono-acetylated (**1**), the di-acetylated regioisomer (**3**), as well as the tri-acetylated (**4**) molecules in order to evaluate their respective biological potential. The synthetic path is shown in Scheme 1 and the results of the reactions are reported in Table 1. The chemical structure, name and Rf values of the various acetylated products are given in Table 2. The acetylating agents used were acetic anhydride or acetyl chloride. Sodium bicarbonate, pyridine and trimethylamine were used as a base in the reaction. As indicated in Table 1, sodium bicarbonate and pyridine were ineffective in providing the desired acetylated products (see entries 1 and 2). However, with a combination of acetic anhydride, trimethylamine in dichloromethane stirred at room temperature for 30 min the mono-acetylated derivative (**1**) was produced with about 48% of as the major product (see entry 3). **DAB-2-28** (**2**) was obtained predominantly with 37% yield using the same reaction conditions but at 40 °C (see entry 4). Also in entry 5, with a longer reaction period, 1 h instead of 30 min, the tri-acetylated material (**4**) was obtained as the major product along with **DAB-2-28** (**2**) with about 28% and 15%, respectively. In entry 6, a mixture of dichloromethane-dimethylsulfoxide (5%) was added to the reaction mixture and stirred for 30 min at 40 °C to yield **DAB-2-28** (**2**) and **4** in about 30% and 10% yield, respectively. However, when flash chromatography was performed immediately at the end of the reaction (entry 7), the di-acetylated derivative **2** was formed with 38% yield and **4** in about 2% yield indicating that further acylation occurs, if the mixture is not readily purified. The cross-acetylated product **3** was more difficult to produce. So in entry 8, using acetyl chloride as a reagent for 2 h at 40 °C led to the formation of **3** along with the tri-acetylated material **4** in 19% and 12%, respectively. Finally, as seen in entry 9, a longer reaction time for the formation of the tri-acetylated derivative **4** did not improve the yield as we observed decomposition during the reaction. Even though the yield of the different acetylated products **1**–**4** is relatively low, they were prepared in sufficient amount to allow the biological study.

Once the optimal reaction conditions to generate **DAB-2-28** (**2**) were discovered (see Table 1, entry 4), they were used to synthesize higher homologs with relevant anhydrides. In each case, the mono-acylated and di-acylated products were isolated. Three additional anhydrides were selected as depicted in Scheme 2 and the results are presented in Table 3. The yield of the mono-acylated products (**1**, **5**, **7**, and **9**) ranged from 0% to 50% and for the di-acylated material (**2**, **6**, **8** and **10**) varied from about 22% to 46%. Interestingly, we observed that the bulkier the anhydride the more mono-acylated and the less di-acylated products were formed which is in agreement with what was expected. Furthermore, the reagents butyric anhydride and isobutyric anhydride necessitate a longer period of reaction time, 0.75 h and 1.5 h, respectively. Only, acetic anhydride, being the less sterically hindered and the more reactive anhydride, led to the formation of tri-acetylated derivative **4** in about 17% yield. All compounds were characterized by their respective infrared (IR), nuclear magnetic resonance spectroscopy (proton and carbon NMR) and by high resolution mass analysis.

3. Results and discussion

3.1. Evaluation of anti-inflammatory and anti-proliferative properties of the structural components of DAB-1 and its derivatives 1–10

Our previous study has shown that the negative effects of **DAB-1** on cell viability would not be caused by an increase in cell mortality but rather by stopping cell proliferation [3,28]. Then, we first evaluate the impact of **DAB-1** derivatives **1**–**10** on NO production and cell viability, separately, in MB49-I cells (Fig. 2A and B). Our results indicate that, in comparison with **DAB-1**, compounds **1**, **2**, **3**, **5**, **7** and **9** were more efficient than compounds **4**, **6**, **8** and **10** to inhibit NO production (Fig. 2A). As shown in Fig. 2B, analysis of different DABs in cell proliferation indicates that compounds **1**, **3**, **5**, and **9** all have a similar inhibitory effect on cell proliferation compared to **DAB-1,** while compounds **2** and **7** being less efficient than **DAB-1** to inhibit cell proliferation. However, compounds **4**, **6**, **8** and **10** all decreased cell proliferation more efficiently than **DAB-1** indicating they are more cytotoxic. Normalization of NO production and NO production inhibition data in relation to the relative number of viable/proliferating cells is reported in Fig. 2C and D.

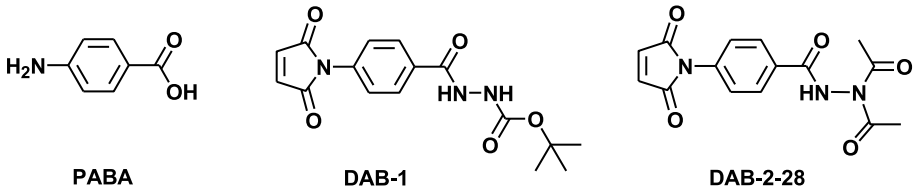

Fig. 1. Structure of **DAB-1** and **DAB-2-28** made from the natural product *para*-aminobenzoic acid (PABA).

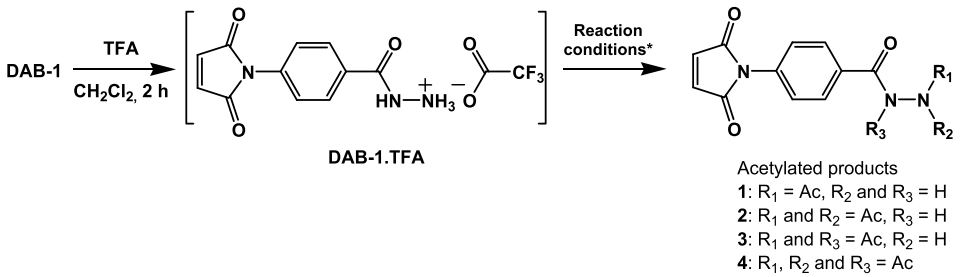

***Reagents and conditions:**
Compound **1**: Table 1, entry 3: Ac_2O, Et_3N, CH_2Cl_2, 22 °C, 0.5 h (48%)
Compound **2**: Table 1, entry 4: Ac_2O, Et_3N, CH_2Cl_2, 40 °C, 0.5 h (37%)
Compound **3**: Table 1, entry 8: AcCl, Et_3N, CH_2Cl_2:DMSO (5%), 40 °C, 2 h (19%)
Compound **4**: Table 1, entry 5: Ac_2O, Et_3N, CH_2Cl_2, 40 °C, 1 h (28%)

Scheme 1. Optimization of the acetylation reaction of **DAB-1** for the production of mono- (**1**), di- (**2** (or **DAB-2-28**) and **3**) and tri-acetylated molecules (**4**).

Table 1
Reaction conditions and yields obtained for the different acetylated **DAB-1** molecules.[a]

Entry #	CH_2Cl_2/DMSO	$(Ac)_2O$ eq.	AcCl eq.	Base eq.	Reaction time	T °C	1[b] Yield	2[b] Yield	3[b,c] Yield	4[b] Yield
1	4 mL/0 mL	5.0 ± 0.1	–	$NaHCO_3$ 3.0	2 h	rt	–	–	–	–
2	4 mL/0 mL	5.0 ± 0.1	–	Pyridine 6.0	0.75 h	rt	–	–	–	–
3	4 mL/0 mL	5.0 ± 0.1	–	Et_3N 4.8	0.5 h	rt	48.5%	11.1%	–	1.4%
4	4 mL/0 mL	5.0 ± 0.1	–	Et_3N 6.0	0.5 h	40 °C	–	36.8%	–	17.3%
5	4 mL/0 mL	5.0 ± 0.1	–	Et_3N 6.0	1 h	40 °C	–	14.6%	–	27.7%
6	4 mL/0.2 mL	5.0 ± 0.1	–	Et_3N 6.0	0.5 h	40 °C	–	30.3%	–	10.5%
7[d]	4 mL/0.2 mL	5.0 ± 0.1	–	Et_3N 6.0	0.5 h	40 °C	–	38.3%	–	1.8%
8	4 mL/0.2 mL	–	6.0 ± 0.1	Et_3N 6.2	2 h	40 °C	–	–	19.4%	11.9%
9	4 mL/0 mL	5.0 ± 0.1	–	Et_3N 6.0	1.5 h	40 °C	–	–	–	9.5%

[a] See Table 2 for the structures of **1**, **2**, **3** and **4**.
[b] Only the major components of the mixture were isolated by flash chromatography.
[c] The di-acetylated product **3** was never formed while using acetic anhydride.
[d] Flash chromatography performed immediately after the reaction.

Table 2
Chemical structure, name and Rf values[a] of the various acetylated **DAB-1** molecules.

1 Mono-acetylated Rf: 0.04	2 Di-acetylated Rf: 0.20	3 Di-acetylated (isomer) Rf: 0.39	4 Tri-acetylated Rf: 0.25
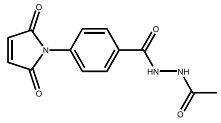	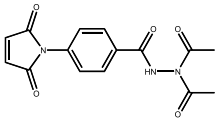	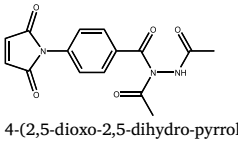	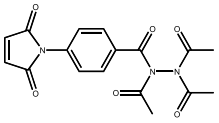
4-(2,5-dioxo-2,5-dihydro-pyrrol-1-yl)-benzoic acid *N′*-acetyl-hydrazide	4-(2,5-dioxo-2,5-dihydro-pyrrol-1-yl)-benzoic acid *N′,N′*-diacetyl-hydrazide	4-(2,5-dioxo-2,5-dihydro-pyrrol-1-yl)-benzoic acid *N,N′*-diacetyl-hydrazide	4-(2,5-dioxo-2,5-dihydro-pyrrol-1-yl)-benzoic acid triacetylhydrazide

[a] Eluent: hexane/acetone: 60/40.

Collectively, these results clearly shown that compounds **1**, **2**, **3**, **4**, **5**, **7**, **8**, **9**, and **10** were more efficient than **DAB-1** to inhibit NO production, with compound **6** having similar effect that **DAB-1** to inhibit NO production (Fig. 2C and D). However, based on statistical analysis, the DABs with the highest rate of inhibition of NO production are the molecules **1** (83%), **3** (79%), **5** (79%), **7** (80%), **9** (81%), compared to molecules **2** (68%), **4** (67%), **6** (62%), **8** (68%) and **10** (74%). In general, SAR of this type of molecule shows the following pattern for NO inhibition: mono-acylated molecules (**1**, **5**, **7**, **9**) > di-acylated molecules (**2**, **6**, **8**, **10**), with the exception of **3,** a di-acetylated analog that displays very good NO inhibitory effects. SAR relative to the cytotoxicity follows this pattern: mono-acylated (**1**, **5**, **7**, **9**) < di-acylated molecules (**6**, **8**, **10**). Interestingly, the tri-acetylated derivative **4** is more toxic than the mono-acetylated (**1**) and the di-acetylated regioisomers (**2** and **3**).

4. Conclusion

In this study, we prepared and characterized several acylated hydrazide molecules designed for the treatment of BCa. They were prepared from **DAB-1** as the starting material. With different reaction conditions

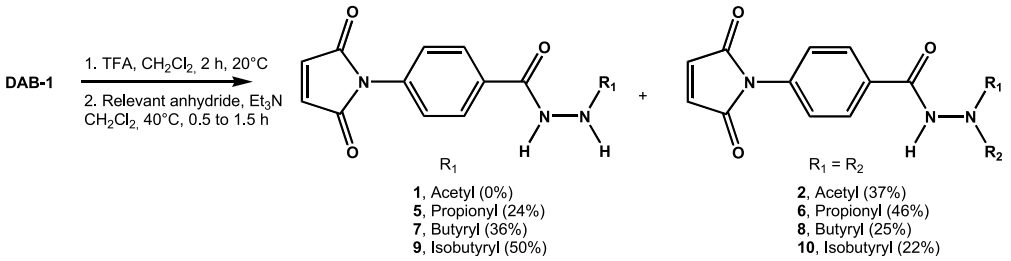

Scheme 2. Reaction of **DAB-1** with various anhydrides to yield higher homologs of **1** (R_1 = Ac) and **2** (R_1 and R_2 = Ac).

Table 3
Results from the reaction of **DAB-1** with anhydride using the best reaction conditions.

Anhydride	Reaction time	T °C	R_1	Yield	$R_1 = R_2$	Yield	Total yield
Acetic anhydride	0.5 h	40 °C	Acetyl (**1**)	0%	Diacetyl (**2**)	36.8%	36.8%[a]
Propionic anhydride	0.5 h	40 °C	Propionyl (**5**)	23.9%	Dipropionyl (**6**)	46.2%	70.1%
Butyric anhydride	0.75 h	40 °C	Butyryl (**7**)	36.7%	Dibutyryl (**8**)	25.5%	62.2%
Isobutyric anhydride	1.5 h	40 °C	Isobutyryl (**9**)	50.0%	Diisobutyryl (**10**)	22.3%	72.3%

[a] The tri-acetylated products **3** was also formed with 17.3% (see Table 1, entry 4).

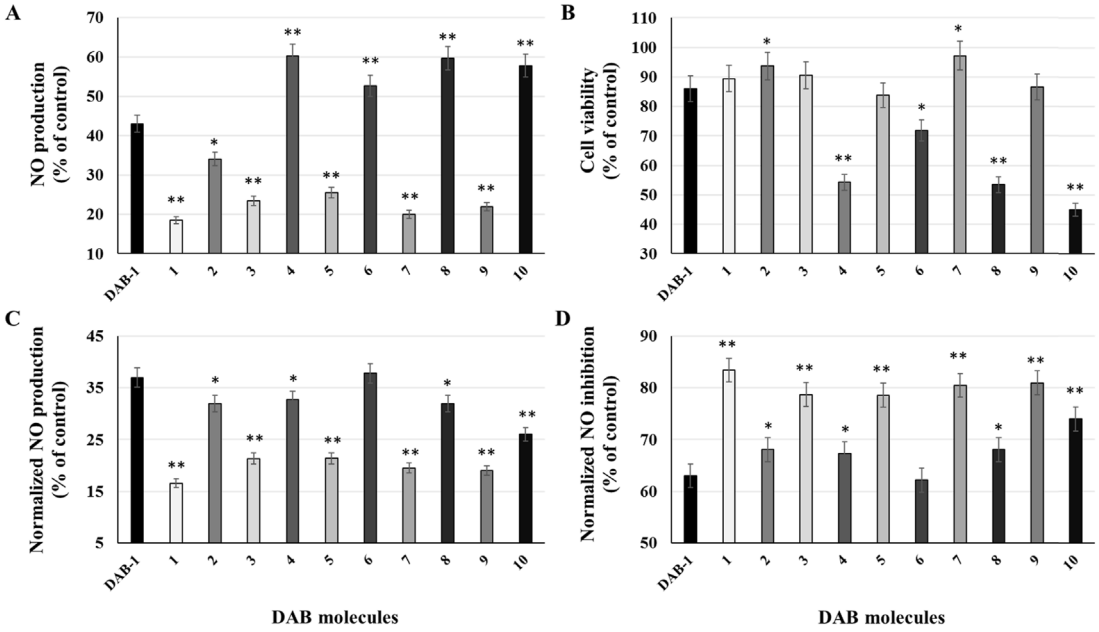

Fig. 2. Regulatory effects of DAB-1 and its derivatives in nitric oxide (NO) production related to cell viability. Murine bladder cancer MB49-I cells were pretreated with **DAB-1** and its derivatives at 20 μM for 30 min, and then washed and activated with IFNγ and TNFα. Cells and supernatants were harvested and prepared for cell viability (MTT assay) and NO measurements (Griess reagent assay) were performed after 24 h of incubation. Data is presented as percent of control for A) NO production, B) Cell viability, C) Normalized NO production, and D) Normalized NO inhibition. $^*p < 0.05$ and $^{**}p < 0.01$ indicated significant difference compared to **DAB-1**.

using acetic anhydride a mono-acetylated (**1**), two di-acetylated regioisomers (**2** and **3**) and a tri-acetylated (**4**) products were obtained allowing comparison of their biological potential. As well, three mono-acylated (**5**, **7** and **9**) and di-acylated (**6**, **8** and **10**) higher homologs were made using relevant anhydrides. It was discovered that generally all mono-acylated derivatives (**1**, **5**, **7** and **9**) were less toxic on murine bladder cancer cells than their corresponding di-acylated homologs (**2**, **6**, **8** and **10**). Interestingly, the di-acetylated compound **3,** regioisomer of **2** possesses very good NO inhibitory activity and displays low toxicity. However, this specific molecule is difficult to synthesize with good yield. In addition, the tri-acetylated derivative **4** shows higher toxicity than the other three acetylated molecules (**1**, **2** and **3**) derived from **DAB-1**. Therefore, from this study, it has been established that the mono-acetylated derivative **1** is the best molecule for further investigations in the future.

5. Experimental protocols

5.1. Biological methods

5.1.1. Evaluation of NO production and cell viability/proliferation

Cell viability and NO production assays were performed along with cultured cells and cell cultured-derived supernatant. Briefly, murine bladder cancer MB49-I cells were seeded into 96-well plate ($7{,}5 \times 10^3$ cells/well) and cultured for 24 h at 37 °C and 5% CO_2. Cells were pre-treated with 0.1% DMSO (control), and **DAB-1** and its derivatives at 20 μM for 60 min, as described [3]. Then, cells were washed and stimulated for a period of 24 h with cytokines IFNγ (5 ng/mL) and TNFα (25 ng/mL).

At the end of stimulation period, cells and supernatants were harvested and prepared for cell viability and NO measurements. As previously described, NO production and cell viability/proliferation were measured by the Griess reagent and the MTT reagent methods, respectively [3]. Data is presented as percent of control (0.1% DMSO) for NO production and cell viability. Data normalization for the levels of NO production and NO production inhibition was computed considering the relative number of viable cells for each condition.

5.1.2. Statistical analyses

Difference between groups was evaluated by two-way ANOVA followed by Bonferonni post-test, as described [19]. Data is presented as means ± SEM from three independent experiments performed in triplicate. Statistical differences were considered to be significant at a value of $p < 0.05$ (*$p < 0.05$, **$p < 0.01$).

5.2. Chemistry

Anhydrous reactions were performed under an inert atmosphere of nitrogen. The starting material, reactant and solvents were obtained commercially and were used as such or purified and dried by standard means [32]. Organic solutions were dried over magnesium sulfate ($MgSO_4$), filtered and evaporated on a rotary evaporator under reduced pressure. All reactions were monitored by UV fluorescence. Commercial TLC plates were Sigma T 6145 (polyester silica gel 60 Å, 0.25 mm). Flash column chromatography was performed according to the method of Still et al. on Merck grade 60 silica gel, 230–400 mesh [33]. All solvents used in chromatography were distilled.

The infrared spectra were taken on a Nicolet Impact 420 FT-IR spectrophotometer. Mass spectral assays were obtained using a MS model 6210, Agilent technology instrument. The high resolution mass spectra (HRMS) were obtained by TOF (time of flight) using ESI (electrospray ionization) using the positive mode (ESI+) (Université du Québec à Montréal). Nuclear magnetic resonance (NMR) spectra were recorded on a Varian 200 MHz NMR apparatus. Samples were dissolved in deuterated acetone (acetone-d_6) or deuterated dimethylsulfoxide (DMSO-d_6) for data acquisition using the residual solvent signal as internal standard (acetone, δ 2.05 ppm for ^{1}H NMR and δ 29.84 ppm for ^{13}C NMR; dimethylsulfoxide, δ 2.50 ppm for ^{1}H NMR and δ 39.52 ppm for ^{13}C NMR). Chemical shifts (δ) are expressed in parts per million (ppm), the coupling constants (J) are expressed in hertz (Hz). Multiplicities are described by the following abbreviations: s for singlet, d for doublet, t for triplet, m for multiplet, #m for several multiplets and, br s for broad singlet.

5.2.1. Synthesis of 4-maleimidylphenyl-hydrazide molecules

5.2.1.1. Synthesis of tert-butyl 2-(4-(2,5-dioxo-2,5-dihydro-1H-pyrrol-1-yl) benzoyl)hydrazinecarboxylate (DAB-1). **DAB-1** was synthesized using a procedure reported in an earlier manuscript [28]. The ^{1}H NMR and ^{13}C NMR spectral data are given to facilitate comparison with the novel molecules reported in this manuscript. ^{1}H NMR (200 MHz, DMSO-d6, δ ppm): 10.25 and 8.93 (2 x s, 2H, 2 x NH), 7.92 and 7.46 (2 x d, $J = 8.4$ Hz, 4H, aromatic), 7.20 (s, 2H, maleimide), 1.41 (s, 9H, 3 x CH_3); ^{13}C NMR (50 MHz, DMSO-d6, δ ppm): 170.1, 165.8, 155.9, 135.3, 135.0, 131.9, 128.4, 126.7, 79.7, 28.5.

5.2.1.2. Synthesis of 4-(2,5-dioxo-2,5-dihydro-pyrrol-1-yl)-benzoic acid hydrazide trifluoroacetic acid salt (DAB-1.TFA). A solution of **DAB-1** (106 mg, 0.32 mmol) dissolved in dichloromethane (1 mL) and trifluoroacetic acid (0.25 mL) was stirred at 20 °C for a period of 2 h. Afterwards, the excess trifluoroacetic acid was removed under vacuum at 20 °C to give compound **DAB-1.TFA** quantitatively. IR (ν, cm^{-1}): 3500-2500 (CO_2H), 3277 (NH), 1710 (C═O); ^{1}H NMR (200 MHz, DMSO-d6, δ ppm): 11.62 (br s, 1H, $N\underline{H}\underline{N}H_3^+CF_3CO_2^-$), 8.63 (br s, NH_3^+), 8.01 and 7.56 (2 x d, $J =$ 8.5 Hz, 4H, aromatic), 7.24 (s, 2H, maleimide); ^{13}C NMR (50 MHz, DMSO-d6, δ ppm): 169.6, 165.4, 135.5, 135.0, 129.4, 128.4, 126.5.

5.2.1.3. Synthesis of N′-acetyl-4-(2,5-dioxo-2,5-dihydro-1H-pyrrol-1-yl) benzohydrazide (1). Acetic anhydride (145 μL, 1.53 mmol) and triethylamine (255 μL, 1.83 mmol) were added to a cooled solution of crude **DAB-1.TFA** (104 mg, 0.30 mmol) dissolved in dichloromethane (4 mL). The mixture was stirred at 20 °C for 30 min. Afterwards, the suspension was filtered on fritted glass filter under vacuum. The product was washed with dichloromethane (4 x 2 mL) and with water (4 x 2 mL) and dried under vacuum to give 40 mg (40%) of the desired material **1**. Yields up to about 48.5% were obtained using this procedure. mp: Decomposition begins at 211 °C; IR (ν, cm^{-1}): 3210 (N–H), 3101-3018 (C–H), 1706 (C═O), 1685 (C═O), 1646 (C═O), 1606 (C═C); ^{1}H NMR (200 MHz, DMSO-d6, δ ppm): 10.34 and 9.91 (2 x s, 2H, 2 x NH), 7.94 and 7.47 (2 x d, $J = 8.2$ Hz, 4H, aromatic), 7.20 (s, 2H, maleimide), 1.91 (s, 3H, CH_3); ^{13}C NMR (50 MHz, DMSO-d6, δ ppm): 170.1, 169.0, 165.3, 135.3, 135.0, 131.9, 128.5, 126.7, 21.1; ESI + HRMS: (M + H)+ calculated for $C_{13}H_{12}N_3O_4 = 274.0822$; found = 274.0818 and ESI + HRMS: (M + Na)+ calculated for $C_{13}H_{11}N_3NaO_4 = 296.0642$; found = 296.0636.

5.2.1.4. Synthesis of N′,N′-diacetyl-4-(2,5-dioxo-2,5-dihydro-1H-pyrrol-1-yl)benzohydrazide (2 or DAB-2-28). Acetic anhydride (0.72 mL, 7.6 mmol) and triethylamine (1.27 mL, 9.1 mmol) were added to a cooled solution (0 °C) of crude **DAB-1.TFA** (523 mg, 1.51 mmol) dissolved in dichloromethane (10 mL). The mixture was stirred at 20 °C for 30 min. Afterwards, the organic phase was diluted with ethyl acetate (75 mL) directly into an extraction funnel. The organic phase was washed with a 5% sodium bicarbonate aqueous solution (2 x 50 mL) and with water (4 x 50 mL). The organic phase was dried with anhydrous magnesium sulfate, filtered and evaporated to the crude material. The product was purified by flash column chromatography using a mixture of hexane/acetone (7/3) to give 86 mg (18%) of the desired material **2**. Of note, using the reaction conditions of entry 4 indicated in Table 1 (40 °C for 30 min), compound **2** was obtained with about 37% yield. mp: Decomposition begins at 190 °C; IR (ν, cm^{-1}): 3194 (NH), 3093-3021 (C–H), 1701 (C═O), 1661 (C═O), 1607 (C═C); ^{1}H NMR (200 MHz, acetone-d6, δ ppm): 10.14 (s, 1H, NH), 8.09 and 7.61 (2 x d, $J = 8.8$ Hz, 4H, aromatic), 7.09 (s, 2H, maleimide), 2.41 (s, 6H, 2 x CH_3); ^{13}C NMR (50 MHz, acetone-d6, δ ppm): 171.1, 169.3, 166.0, 135.8, 134.7, 130.8, 128.2, 126.1, 24.2; ESI + HRMS: (M + H)+ calculated for $C_{15}H_{14}N_3O_5 = 316.0928$; found = 316.0945 and ESI + HRMS: (M + H -Ac)+ calculated for $C_{13}H_{12}N_3O_4 = 275.08252$; found = 275.0856.

5.2.1.5. Synthesis of N,N′-diacetyl-4-(2,5-dioxo-2,5-dihydro-1H-pyrrol-1-yl)benzohydrazide (3). Acetyl chloride (130 μL, 1.83 mmol) and triethylamine (260 μL, 1.87 mmol) were added to a cooled solution of crude **DAB-1-TFA** (104 mg, 0.30 mmol) dissolved in dichloromethane (4 mL) and DMSO (0.2 mL). The mixture was stirred at 40 °C for 2 h. Afterwards, the crude product was directly adsorbed on silica and purified by flash column chromatography using a mixture of hexane/acetone (4/1) to give 18.5 mg (19%) of the desired material **3**. mp: Decomposition begins at 159 °C; IR (ν, cm^{-1}): 3397 (N–H), 3163-2944 (C–H), 1783 (C═O), 1711 (C═O), 1652 (C═O), 1613 (C═C); ^{1}H NMR (200 MHz, $(CD_3)_2CO$, δ ppm): 8.00 and 7.65 (2 x d, $J = 8.8$ Hz, 4H, aromatic), 7.10 (s, 2H, maleimide), 2.35 and 2.21 (2 x s, 6H, 2 x CH_3); ^{13}C NMR (50 MHz, $(CD_3)_2CO$, δ ppm): 169.2, 168.4, 166.5, 150.8, 135.7, 134.7, 127.1, 126.5, 121.2, 21.8, 19.9.

5.2.1.6. Synthesis of N,N′,N′-triacetyl-4-(2,5-dioxo-2,5-dihydro-1H-pyrrol-1-yl)benzohydrazide (4). Acetic anhydride (140 μL, 1.48 mmol) and triethylamine (250 μL, 1.79 mmol) were added to a cooled solution of crude **DAB-1.TFA** (104 mg, 0.30 mmol) dissolved in dichloromethane (4 mL). The mixture was stirred at 40 °C for 60 min. Afterwards, the crude product was directly adsorbed on silica and purified by flash column

chromatography using a mixture of hexane/acetone (4/1) to give 30.1 mg (28%) of the desired material **4**. mp: 165.2–166.0 °C; IR (ν, cm^{-1}): 3092-2936 (C–H), 1744 (C═O), 1706 (C═O), 1605 (C═C); ^{1}H NMR (200 MHz, $(CD_3)_2CO$, δ ppm): 7.84 and 7.58 (2 x d, J = 8.6 Hz, 4H, aromatic), 7.09 (s, 2H, maleimide), 2.44 and 2.34 (2 x s, 9H, 3 x CH_3); ^{13}C NMR (50 MHz, $(CD_3)_2CO$, δ ppm): 171.3, 170.9, 169.4, 169.2, 135.6, 134.7, 132.8, 128.7, 125.6, 24.0 23.3; ESI + HRMS: (M + Na)+ calculated for $C_{17}H_{15}N_3NaO_6$ = 380.0853; found = 380.0852.

5.2.1.7. Synthesis of 4-(2,5-dioxo-2,5-dihydro-1H-pyrrol-1-yl)-N′-propionylbenzohydrazide (5) and 4-(2,5-dioxo-2,5-dihydro-1H-pyrrol-1-yl)-N′,N′-dipropionylbenzohydrazide (6). Propionic anhydride (200 μL, 1.56 mmol) and triethylamine (250 μL, 1.79 mmol) were added to a cooled solution of crude **DAB-1-TFA** (104 mg, 0.30 mmol) dissolved in dichloromethane (4 mL). The mixture was stirred at 40 °C for 30 min. Afterwards, the crude products were directly adsorbed on silica and purified and separated by flash column chromatography using a mixture of hexane/acetone (4/1) to give **5** (20.9 mg, 24%) and **6** (48.3 mg, 46%). Compound **5**: mp: Decomposition begins at 205 °C; IR (ν, cm^{-1}): 3288 and 3231 (2 x N–H), 3093-2882 (C–H), 1703 (C═O), 1677 (C═O), 1623 (C═O), 1586 (C═C); ^{1}H NMR (200 MHz, $(CD_3)_2SO$, δ ppm): 10.05 and 9.85 (2 x s, 2H, 2 x NH), 7.95 and 7.47 (2 x d, J = 8.6 Hz, 4H, aromatic), 7.21 (s, 2H, maleimide), 2.19 (q, J = 7.5 Hz, 2H, CH_2), 1.05 (t, J = 7.5 Hz, 3H, CH_3); ^{13}C NMR (50 MHz, $(CD_3)_2SO$, δ ppm): 172.7, 170.1, 165.3, 135.3, 135.0, 131.9, 128.5, 126.7, 27,0, 10.1; ESI + HRMS: (M + H)+ calculated for $C_{14}H_{14}N_3O_4$ = 288.0979; found = 288.0969 and ESI + HRMS: (M + Na)+ calculated for $C_{14}H_{13}N_3NaO_4$ = 310.0798; found = 310.0785. Compound **6**: mp: 174.1–174.8 °C; IR (ν, cm^{-1}): 3283 (N–H), 3094-2880 (C–H), 1705 (C═O), 1664 (C═O), 1610 (C═C); ^{1}H NMR (200 MHz, $(CD_3)_2CO$, δ ppm): 10.05 (s, 1H, NH), 8.09 and 7.61 (2 x d, J = 8.8 Hz, 4H, aromatic), 7.09 (s, 2H, maleimide), 2.85–2.81 (m, 4H, 2 x CH_2), 1.10 (t, J = 7.4 Hz, 6H, 2 x CH_3); ^{13}C NMR (50 MHz, $(CD_3)_2CO$, δ ppm): 174.7, 169.3, 166.1, 135.8, 134.7, 130.9, 128.2, 126.1, 29.8, 8.1; ESI + HRMS: (M + Na)+ calculated for $C_{17}H_{17}N_3NaO_5$ = 366.1060; found = 366.1052.

5.2.1.8. Synthesis of N′-butyryl-4-(2,5-dioxo-2,5-dihydro-1H-pyrrol-1-yl) benzohydrazide (7) and N′,N′-dibutyryl-4-(2,5-dioxo-2,5-dihydro-1H-pyrrol-1-yl)benzohydrazide (8). Butyric anhydride (250 μL, 1.53 mmol) and triethylamine (250 μL, 1.79 mmol) were added to a cooled solution of crude **DAB-1.TFA** (104 mg, 0.30 mmol) dissolved in dichloromethane (4 mL). The mixture was stirred at 40 °C for 45 min. Afterwards, the crude products were directly adsorbed on silica and purified and separated by flash column chromatography using a mixture of hexane/acetone (4/1) to give **7** (33.6 mg, 37%) and **8** (28.7 mg, 25%). Compound **7**: mp: Decomposition begins at 200 °C; IR (ν, cm^{-1}): 3335 and 3262 (2 x N–H), 3117-2875 (C–H), 1715 (C═O), 1687 (C═O), 1620 (C═O), 1572 (C═C); ^{1}H NMR (200 MHz, $(CD_3)_2SO$, δ ppm): 10.05 and 9.85 (2 x s, 2H, 2 x NH), 7.95 and 7.47 (2 x d, J = 8.2 Hz, 4H, aromatic), 7.21 (s, 2H, maleimide), 2.15 (t, J = 7.3 Hz, 2H, CH_2 α), 1.57 (sex, J = 7.3 Hz, 2H, CH_2 β) 0.91 (t, J = 7.3 Hz, 3H, CH_3); ^{13}C NMR (50 MHz, $(CD_3)_2SO$, δ ppm): 171.9, 170.1, 165.3, 135.3, 135.0, 131.9, 128.5, 126.7, 35.7, 19.0, 14.0; ESI + HRMS: (M + H)+ calculated for $C_{15}H_{16}N_3O_4$ = 302.1135; found = 302.1129 and ESI + HRMS: (M + Na)+ calculated for $C_{15}H_{15}N_3NaO_4$ = 324.0955; found = 324.0946. Compound **8**: mp: 166.3–167.0 °C; IR (ν, cm^{-1}): 3273 (N–H), 3093-2875 (C–H), 1704 (C═O), 1666 (C═O), 1609 (C═C); ^{1}H NMR (200 MHz, $(CD_3)_2CO$, δ ppm): 10.06 (s, 1H, NH), 8.09 and 7.61 (2 x d, J = 8.8 Hz, 4H, aromatic), 7.09 (s, 2H, maleimide), 2.85–2.81 (m, 4H, 2 x CH_2 α), 1.66 (sex, J = 7.4 Hz, 4H, 2 x CH_2 β), 0.95 (t, J = 7.4 Hz, 6H, 2 x CH_3); ^{13}C NMR (50 MHz, $(CD_3)_2CO$, δ ppm): 173.8, 169.3, 166.1, 135.8, 134.7, 130.9, 128.2, 126.1, 38.2, 17.6, 13.0; ESI + HRMS: (M + Na)+ calculated for $C_{19}H_{21}N_3NaO_5$ = 394.1373; found = 394.1367.

5.2.1.9. Synthesis of 4-(2,5-dioxo-2,5-dihydro-1H-pyrrol-1-yl)-N′-isobutyrylbenzohydrazide (9) and 4-(2,5-dioxo-2,5-dihydro-1H-pyrrol-1-yl)-N′,N′-diisobutyrylbenzohydrazide (10). Isobutyric anhydride (250 μL, 1.51 mmol) and triethylamine (250 μL, 1.79 mmol) were added to a cooled solution of crude **DAB-1.TFA** (104 mg, 0.30 mmol) dissolved in dichloromethane (4 mL). The mixture was stirred at 40 °C for 90 min. Afterwards, the crude products were directly adsorbed on silica and purified and separated by flash column chromatography using a mixture of hexane/acetone (4/1) to give **9** (45.8 mg, 50%) and **10** (25.2 mg, 22%). Compound **9**: mp: Decomposition begins at 208 °C; IR (ν, cm^{-1}): 3301 and 3232 (2 x N–H), 3087-2876 (C–H), 1705 (C═O), 1681 (C═O), 1630 (C═O), 1584 (C═C); ^{1}H NMR (200 MHz, $(CD_3)_2SO$, δ ppm): 10.36 and 9.85 (2 x s, 2H, 2 x NH), 7.95 and 7.47 (2 x d, J = 8.8 Hz, 4H, aromatic), 7.21 (s, 2H, maleimide), 2.53–2.47 (m, 1H, CH), 1.07 (d, J = 7.0 Hz, 6H, 2 x CH_3); ^{13}C NMR (50 MHz, $(CD_3)_2SO$, δ ppm): 176.0, 170.1, 165.3, 135.3, 135.0, 132.0, 128.5, 126.7, 32.6, 19.8; ESI + HRMS: (M + H)+ calculated for $C_{15}H_{16}N_3O_4$ = 302.1135; found = 302.1130 and ESI + HRMS: (M + Na)+ calculated for $C_{15}H_{15}N_3NaO_4$ = 324.0955; found = 324.0948. Compound **10**: mp: 169.5–170.5 °C; IR (ν, cm^{-1}): 3275 (N–H), 3091-2878 (C–H), 1705 (C═O), 1672 (C═O), 1609 (C═C); ^{1}H NMR (200 MHz, $(CD_3)_2CO$, δ ppm): 10.09 (s, 1H, NH), 8.09 and 7.61 (2 x d, J = 8.8 Hz, 4H, aromatic), 7.09 (s, 2H, maleimide), 3.45 (sep, J = 6,8 Hz, 2H, 2 x CH), 1.17 (d, J = 6.8 Hz, 12H, 4 x CH_3); ^{13}C NMR (50 MHz, $(CD_3)_2CO$, δ ppm): 178.5, 169.3, 166.5, 135.8, 134.7, 130.9, 128.2, 126.1, 34.1, 18.6; ESI + HRMS: (M + Na)+ calculated for $C_{19}H_{21}N_3NaO_5$ = 394.1373; found = 394.1369.

Declaration of competing interest

The authors declare that they have no known competing financial interests or personal relationships that could have appeared to influence the work reported in this paper.

Acknowledgments

The authors thank the Cancer Research Society (CRS: number 22471) and the Canadian Institutes of Health Research for financial support (CIHR; number 392334). This work was also sponsored by a grant from Aligo Innovation (number 150923), the "*Ministère de l'Économie et de l'Innovation*", Québec Government to C. Reyes-Moreno and G. Bérubé, and by the Natural Sciences and Engineering Research Council of Canada (NSERC) to H.A. Tajmir-Riahi (NSERC; number 1512). Y. Oufqir obtained a M.Sc. scholarship from the CIHR. L. Fortin holds a M.Sc. scholarship from the Fonds de la Recherche en Santé du Québec (FRSQ).

Appendix A. Supplementary data

Supplementary data to this article can be found online at https://doi.org/10.1016/j.ejmcr.2022.100064.

References

[1] L. Falzone, S. Salomone, M. Libra, Evolution of cancer pharmacological treatments at the turn of the third millennium, Front. Pharmacol. 9 (2018) 1300.
[2] T. Briolay, T. Petithomme, M. Fouet, N. Nguyen-Pham, C. Blanquart, N. Boisgerault, Delivery of cancer therapies by synthetic and bio-inspired nanovectors, Mol. Cancer 20 (55) (2021) 1–24.
[3] A.B. Kunnumakkara, D. Bordoloi, B.L. Sailo, N.K. Roy, K.K. Thakur, K. Banik, M. Shakibaei, S.C. Gupta, B.B. Aggarwal, Cancer drug development: the missing links, Exp. Biol. Med. 244 (2019) 663–689.
[4] O.M. Soltan, M.E. Shoman, S.A. Abdel-Aziz, A. Narumi, H. Konno, M. Abdel-Aziz, Molecular hybrids: a five-year survey on structures of multipletargeted hybrids of protein kinase inhibitors for cancer therapy, Eur. J. Med. Chem. 225 (2021) 113768, 1–32.
[5] K. Nepali, S. Sharma, M. Sharma, P.M. Bedi, K.L. Dhar, Rational approaches, design strategies, structure activity relationship and mechanistic insights for anticancer hybrids, Eur. J. Med. Chem. 77 (2014) 422–487.
[6] C. Viegas-Junior, A. Danuello, V. da Silva Bolzani, E.J. Barreiro, C.A.M. Fraga, Molecular hybridization: a useful tool in the design of new drug prototypes, Curr. Med. Chem. 14 (2007) 1829–1852.
[7] S. Fortin, G. Bérubé, Advances in the development of hybrid anticancer drugs, Expet Opin. Drug Discov. 8 (2013) 1029–1047.

[8] G. Bérubé, An overview of molecular hybrids in drug discovery, Expet Opin. Drug Discov. 11 (2016) 281–305.
[9] S. Mishra Shaveta, P. Singh, Hybrid molecules: the privileged scaffolds for various pharmaceuticals, Eur. J. Med. Chem. 124 (2016) 500–536.
[10] C.G. Arya, R. Gondru, Y. Li, J. Banothu, Coumarine-benzimidazole hybrids: a review of developments in medicinal chemistry, Eur. J. Med. Chem. 227 (2022) 1–18, 113921.
[11] K. Tilekar, O. Shelke, N. Upadhyay, A. Lavecchia, C.S. Ramaa, Current status and future prospects of molecular hybrids with thiazolidinedione (TZD) scaffold in anticancer drug discovery, J. Mol. Struct. 1250 (Part 2) (2022) 1–18, 131767.
[12] N. Micale, M.S. Molonia, A. Citarella, F. Cimino, A. Saija, M. Cristani, A. Speciale, Natural product-based hybrids as potential candidates for the treatment of cancer: focus on curcumin and resveratrol, Molecules 26 (2021) 1–34, 4665.
[13] G. Teli, P.A. Chawla, Hybridization of imidazole with various heterocycles in targeting cancer: a decade's work, ChemistrySelect 6 (2021) 4803–4836.
[14] H. Sung, J. Ferlay, R.L. Siegel, M. Laversanne, I. Soerjomataram, A. Jemal, F. Bray, Global cancer statistics 2020: GLOBOCAN estimates of incidence and mortality worldwide for 36 cancers in 185 countries, Ca - Cancer J. Clin. (2021) 1–41.
[15] D.R. Brenner, H.K. Weir, A.A. Demers, L.F. Ellison, C. Louzado, A. Shaw, D. Turner, R.R. Woods, L.M. Smith, Projected estimates of cancer in Canada in 2020, CMAJ (Can. Med. Assoc. J.) 192 (2020) E199–E205.
[16] P. Li, J. Chen, H. Miyamoto, Androgen receptor signaling in bladder cancer, Cancers 9 (2017) 20.
[17] X. Huang, T. Pan, L. Yan, T. Jin, R. Zhang, B. Chen, J. Feng, T. Duan, Y. Xiang, M. Zhang, X. Chen, Z. Yang, W. Zhang, X. Ding, T. Xie, X. Sui, The inflammatory microenvironment and the urinary microbiome in the initiation and progression of bladder cancer, Genes Dis. 8 (2021) 781–797.
[18] X. Sui, L. Lei, L. Chen, T. Xie, X. Li, Inflammatory microenvironment in the initiation and progression of bladder cancer, Oncotarget 8 (2017) 93279–93294.
[19] J. Girouard, D. Belgorosky, J. Hamelin-Morrissette, V. Boulanger, E. D'orio, D. Ramla, R. Perron, L. Charpentier, A.-M. Eiján, G. Bérubé, C. Reyes-Moreno, Molecular therapy with derivatives of amino benzoic acid inhibits tumor growth and metastasis in murine models of bladder cancer through inhibition of TNFα/NFκB and iNOS/NO pathways, Biochem. Pharmacol. 176 (2020) 1–15, 113778.
[20] M. Dufresne, G. Dumas, É. Asselin, C. Carrier, M. Pouliot, C. Reyes-Moreno, Pro-inflammatory type-1 and anti-inflammatory type-2 macrophages differentially modulate cell survival and invasion of human bladder carcinoma T24 cells, Mol. Immunol. 48 (2011) 1556–1567.
[21] D.B. Thompson, L.E. Siref, M.P. Feloney, R.J. Hauke, D.K. Agrawal, Immunological basis in the pathogenesis and treatment of bladder cancer, Expet Rev. Clin. Immunol. 11 (2015) 265–279.
[22] Z. Zhu, Z. Shen, C. Xu, Inflammatory pathways as promising targets to increase chemotherapy response in bladder cancer, Mediat. Inflamm. 2012 (2012) 528690.
[23] D. Belgorosky, Y. Langle, B. Prack Mc Cormick, L. Colombo, E. Sandes, A.M. Eijan, Inhibition of nitric oxide is a good therapeutic target for bladder tumors that express iNOS, Nitric Oxide 36 (2014) 11–18.
[24] A.W. Chung, K. Anand, A.C. Anselme, A.A. Chan, N. Gupta, L.A. Venta, M.R. Schwartz, W. Qian, Y. Xu, L. Zhang, J. Kuhn, T. Patel, A.A. Rodriguez, A. Belcheva, J. Darcourt, J. Ensor, E. Bernicker, P.-Y. Pan, S.H. Chen, D.J. Lee, P.A. Niravath, J.C. Chang, A phase 1/2 clinical trial of the nitric oxide synthase inhibitor L-NMMA and taxane for treating chemoresistant triple-negative breast cancer, Sci. Transl. Med. 13 (2021), eabj5070.
[25] K. Nakamura, M.J. Smyth, Targeting cancer-related inflammation in the era of immunotherapy, Immunol, Cell Biol. 95 (2017) 325–332.
[26] S.A.K. amadi, A. Bilsland, A.G. Georgakilas, A. Amedei, A. Amin, A. Bishayee, A.S. Azmi, B.L. Lokeshwar, B. Grue, C. Panis, C.S. Boosani, D. Poudyal, D.M. Stafforini, D. Bhakta, E. Niccolai, G. Guha, H.P.V. Rupasinghe, H. Fujii, K. Honoki, K. Mehta, K. Aquilano, L. Lowe, L. J Hofseth, L. Ricciardiello, M.R. Ciriolo, N. Singh, R.L. Whelan, R. Chaturvedi, S.S. Ashraf, H.M.C.S. Kumara, S. Nowsheen, S.I. Mohammed, W.N. Keith, W.G. Helferich, X. Yang, A multi-targeted approach to suppress tumor-promoting inflammation, Semin. Cancer Biol. 35 (Suppl) (2015) S151–S184.
[27] G. Dumas, M. Dufresne, É. Asselin, J. Girouard, C. Carrier, C. Reyes-Moreno, CD40 pathway activation reveals dual function for macrophages in human endometrial cancer cell survival and invasion, Cancer Immunol. Immunother. 62 (2013) 273–283.
[28] J. Hamelin-Morrissette, S. Cloutier, J. Girouard, D. Belgorosky, A.-M. Eiján, J. Legault, C. Reyes-Moreno, G. Bérubé, Identification of an anti-inflammatory derivative with anti-cancer potential: the impact of each of its structural components on inflammatory responses in macrophages and bladder cancer cells, Eur. J. Med. Chem. 96 (2015) 259–269.
[29] P. Chanphai, F. Cloutier, Y. Oufqir, M.-F. Leclerc, A.M. Eiján, C. Reyes-Moreno, G. Bérubé, H.A. Tajmir-Riahi, Biomolecular study and conjugation of two *para*-aminobenzoic acid derivatives with serum proteins: drug binding efficacy and protein structural analysis, J. Biomol. Struct. Dyn. 39 (2021) 79–90.
[30] G. Bérubé, C. Reyes-Moreno, Aminobenzoic acid derivatives for use as anti-inflammatory agents, anti-metastatic agents and/or anticancer agents (WO2017/177316 A1), in: 3R Valo Patent Agent, Bereskin & Parr, 2017.
[31] Y. Oufqir, L. Fortin, J. Girouard, F. Cloutier, M. Cloutier, M.-F. Leclerc, D. Belgorosky, A.M. Eiján, G. Bérubé, C. Reyes-Moreno, Synthesis of new *para*-aminobenzoic acid derivatives, *in vitro* biological evaluation and preclinical validation of DAB-2-28 as a therapeutic option for the treatment of bladder cancer, Eur. J. Med. Chem. Rep..
[32] W.L.F. Armarego, Purification of Laboratory Chemicals, Eight Edition, Butterworth-Heinemann, Oxford, 2017, ISBN 9780128054574, p. 1198.
[33] W.C. Still, M. Kahn, A. Mitra, Rapid chromatographic technique for preparative separations with moderate resolution, J. Org. Chem. 43 (1978) 2923–2925.